CHALMERS

Amin Rasam

A Hybrid LES - Thin Boundary Layer Equations Method for Simulation of Attached and Recirculating Flows

Department of Applied Mechanics
Division of Fluid Dynamics
Chalmers University of Technology
Göteborg Sweden, 2008

Master's Thesis [2007 : 19]

Master's Thesis 2007:19

A Hybrid LES - Thin Boundary Layer Equations Method for Simulation of Attached and Recirculating Flows

Master's Thesis

Amin Rasam

Department of Applied Mechanics
Division of Fluid Dynamics
Chalmers University of Technology
Göteborg, Sweden, 2008

A Hybrid LES - Thin Boundary Layer Equations Method for Simulation of Attached and Recirculating Flows
Master's Thesis
Amin Rasam

Master's Thesis 2007:19
ISSN: 1652-8557

Department of Applied Mechanics,
Division of Fluid Dynamics
Chalmers University of Technology
Se-412 96 Göteborg, Sweden
Phone +46-(0)31-7721400
Fax: +46-(0)31-180976

Printed at Chalmers Reproservice
Göteborg, Sweden 2008

Amin Rasam

Master's Thesis

by

Amin Rasam

rasam@student.chalmers.se

Department of Applied Mechanics

Division of Fluid Dynamics

Chalmers University of Technology

Abstract

In this work, simplified Navier-Stokes equations using thin boundary layer approximations are used as a tool to provide large eddy simulations with proper reliable wall boundary conditions. The usual restriction of using LES in near-wall regions where the scales of turbulence break down to very small scales, usually comparable to wall distance, is the motivation for implementing such hybrid schemes which result in a considerable cut down on computational resources needed and therefore faster simulations, while accuracy can still be maintained in a satisfactory level. In this investigation, turbulent thin boundary layer equations are implemented to a large eddy simulation in-house code used for simulations of incompressible flows. The resulted hybrid scheme is applied to a benchmark case. The case investigated is the fully developed channel flow. The results obtained are compared to Log-Law and DNS of channel flow. A brief discussion about different terms in the boundary layer equations and their role in the accuracy of the results is carried out. Several simulations are done and several interesting features are pointed out including the performance of the method at high Reynolds numbers and the effect of matching point location which is important for hybrid schemes. Also, the sensitivity of the simulations to the eddy viscosity formulation is investigated by applying a number of different formulations including two zero and a one equation model. At the end, a CPU time comparison between different simulations using different eddy viscosity models has also been made.

Keywords: Hybrid Scheme, LES, Thin Boundary Layer, Channel Flow

Acknowledgement

Lots of people really helped me a lot to finish this piece of work. I would like to thank them all. I would like to thank Prof. Lars Davidson for his helps and supports, besides very useful discussions, which made this work possible. Also, His helps in providing me with his LES code besides his many technical comments that helped me figure out its structure is truly appreciated.

Dr. Gunnar Johansson is very much acknowledged for helping me get into the turbulence program and solving many of my problems that otherwise could not be solved. Many thanks to Prof. Lars-Erik Eriksson for his extra time discussions on Aero-acoustics.

I would like to thank lots of people at the mechanical engineering department especially Ulla Lindberg-Thieme, Farzad Shiri, Mohammad Irannezhad and Lei Xu.

I am grateful in depth to the helps of Zeinab's parents, Soheila and Hashem and my parents, Mahboobeh and Ali during my studies.

The most important part of my acknowledgment goes to my dedicated wife, Zeinab. Without your helps, understanding, supports and encouragements I could not succeed to finish my study in Sweden, wish you all the best in life.

Nomenclature

Upper-case Roman

A	Van-Driest constant
J	Jacobian of transformation
I, J, K	Node numbers in x, y and z direction
P_k	Turbulence production term
P, Q	Grid generation forcing terms
P_m	Free stream pressure
Re_τ	Reynolds number based on shear velocity
K	Turbulent kinetic energy
U_{mi}	First LES node velocity
U_*	Wall shear veolcity

Lower-case Roman

e	Nepper Number
p, q, r, s	Grid generation forcing terms
t	Time
u, v, w	Velocity components
u_τ	Friction velocity
x, y, z	Cartesian directions
y_m	y Matching point distance
y^+	y distance in wall units

Lower-case Greek

α, β, γ	Grid generation parameters
ν	Kinematic viscosity
ν_t	Turbulent eddy viscosity
ξ, η	Computational space variables
δ	Channel half width
κ	Von Karman constant
$\xi_x, \xi_y, \eta_x, \eta_y$	Metrics of transformation

Abbreviations

LES	Large eddy simulation

RANS	Reynolds averaged Navier Stokes
Re	Reynolds number
SOR	Successive over relaxation
TBLE	Thin boundary layer equations

Subscripts

i	Direction, node number
w	Wall

Superscripts

$.'$	Denotes a dummy variable

Symbols

$\widetilde{.}$	Spatial filtering
$\sim$	Approximation

Contents

Chapter 1

Introduction

Nowadays, LES[1] has become a very popular tool to deal with certain turbulent problems and is going to become a good replacement for RANS[2] models as the computers become more powerful.

If we make a comparison between LES and RANS in terms of computational cost, LES is about 50-500 times more expensive than the conventional RANS models [1] (depending on the geometry), but if we compare them in terms of accuracy and capabilities LES is much superior to RANS especially in large scale dominated flows. The reason is that we use modeling for fewer scales of motion while in RANS we model all the turbulent scales. But, there are still some difficulties with problems involving walls. As we get close to the walls, the scales of turbulence are reduced to smaller scales, therefore we need more resolution to capture what is going on and that is a drawback for LES, because computational expenses grow dramatically, getting close to DNS[3].

Consider the simple channel flow, as an example. It is estimated that the number of grid points needed to resolve a channel flow properly with LES, scales approximately as: Re_τ^2 [2]. Almost all of the points have to be clustered near the surface and the time step used should also be reduced very much. For example, for a channel flow with a fairly moderate friction Reynolds number of $Re_\tau = 1000$, 70% of the grid points has to be located near wall locations, while this area is only 10% of the channel cross section [1].

This problem has made engineers to invent and try to implement models for near wall regions in LES simulations. One of the early attempts was made by Deardorff [3], who implemented wall functions as a near wall model for LES. This approach works fairly good for non-separating flows and has

[1]Large Eddy Simulation
[2]Reynolds Averaged Navier Stokes
[3]Direct Numerical Simulation

some restrictions. Another approach is to use hybrid schemes [4]. In hybrid schemes, the core flow is resolved using LES with coarse mesh and the near wall region is modeled using unsteady RANS models. Therefore the boundary condition for the LES is provided by URANS and vice versa.

Implementation of a subdivision of hybrid schemes to large eddy simulations is the topic of this project. In this effort, approximate thin boundary layer equations (TBLE) are solved with different turbulence models such as different zero equations and a one equation model. This approach is implemented to the CALC-BFC [4] code and simulations have been done for the case of a channel flow for different Reynolds numbers. A comparison to the universal log-law is made and the benefits of the method are pointed out in terms of CPU time. This is followed by a discussion of importance of different terms in the TBLE.

[4]In-house code, developed for solving incompressible three-dimensional flows

Chapter 2

Large eddy simulation

2.1 Introduction

Large eddy simulation, or LES in short, was first proposed in 1960s and used later by Josef Smagorinsky for meteorological applications. The idea of the method is to resolve the non-isotropic large scales, which depend on the shape of boundaries and flow characteristics, and to model the remaining small scales, which are assumed to be isotropic and can be modeled without loosing much information by introducing an element of modeling using an eddy viscosity model.

2.2 Governing equations

Incompressible Navier Stokes equations in three dimensions along with the continuity equation can be written in the following form:

$$\frac{\partial u_i}{\partial t} + \frac{\partial u_i u_j}{\partial u_j} = -\frac{1}{\rho}\frac{\partial p}{\partial x_i} + \nu\frac{\partial^2 u_i}{\partial x_j \partial x_j}, \quad i = 1, 2, 3 \tag{2.1}$$

$$\frac{\partial u_i}{\partial x_i} = 0 \tag{2.2}$$

where Einstein summation convention is applied over the repeated indices in every expression. Filtering Eq. (2.1) in space gives:

$$\frac{\partial \overline{u}_i}{\partial t} + \frac{\partial \overline{u_i u_j}}{\partial u_j} = -\frac{1}{\rho}\frac{\partial \overline{p}}{\partial x_i} + \nu\frac{\partial^2 \overline{u}_i}{\partial x_j \partial x_j} \tag{2.3}$$

or:

$$\frac{\partial \overline{u}_i}{\partial t} + \frac{\partial \overline{u}_i \overline{u}_j}{\partial u_j} = -\frac{1}{\rho}\frac{\partial \overline{p}}{\partial x_i} + \nu\frac{\partial^2 \overline{u}_i}{\partial x_j \partial x_j} - \frac{\partial \tau_{ij}}{\partial x_j} \tag{2.4}$$

where:

$$\tau_{ij} = \overline{u_i u_j} - \overline{u}_i \overline{u}_j \tag{2.5}$$

τ_{ij} is the effect of unresolved turbulence which is called sub-grid scale (SGS) turbulence. It is assumed that the eddies in the SGS level are isotropic and are modeled as follows:

$$\tau_{ij} - \frac{2}{3}\delta_{ij}\tau_{kk} = -2\nu_t \overline{S}_{ij} \tag{2.6}$$

where the filtered rate of strain tensor is:

$$\overline{S}_{ij} = \frac{1}{2}\left(\frac{\partial \overline{u}_i}{\partial x_j} + \frac{\partial \overline{u}_j}{\partial x_i}\right) \tag{2.7}$$

2.3 Sub-grid scale modeling in the LES region

The sub-grid scale model used here in the LES region is based on the following formulation of the sub-grid scale turbulent kinetic energy (see[5]):

$$\begin{aligned} &\frac{\partial k}{\partial t} + \frac{\partial \overline{u}_j k}{\partial x_j} = \frac{\partial}{\partial x_j}\left[(\nu + \nu_t)\frac{\partial k}{\partial x_j}\right] + P_k - C_\epsilon \frac{k^{3/2}}{l} \\ &P_k = -\tau_{ij}\overline{S}_{ij}, \quad \tau_{ij} = -2\nu_T \overline{S}_{ij} \\ &\nu_t = 0.07\sqrt{K}l, \quad C_\epsilon = 1.05 \\ &l = (\Delta_x \Delta_y \Delta_z)^{1/3} \end{aligned} \tag{2.8}$$

2.4 Numerical method

In the simulations here, we have used finite volume technique in a body fitted coordinate system [6]. When finite volume techniques are used, an implicit filtering is automatically applied, therefore an explicit filtering is not required. When Eq. (2.1) is discretized it becomes:

$$\overline{u}_i^{n+1} = \overline{u}_i^n + \Delta t H\left(\overline{u}_i^n, \overline{u}_i^{n+1}\right) - \frac{1}{\rho}\alpha \Delta t \frac{\partial \overline{p} n+1}{\partial x_i} - \frac{1}{\rho}(1-\alpha)\Delta t \frac{\partial \overline{u}^n}{\partial x_i} \tag{2.9}$$

Here, $H\left(\overline{u}_i^n, \overline{u}_i^{n+1}\right)$ includes convection and viscous as well as subgrid stresses. α is set to 0.5 for the second order Crank-Nicholson time discretization scheme. Second order central differences are used for spatial discretization

of all terms containing spatial differentiations. Solution of Eq. (2.9) will not satisfy continuity. Therefore, an intermediate velocity field is computed by subtracting the implicit part of the pressure gradient. This gives:

$$\overline{u}_i^* = \overline{u}_i^{n+1} + \frac{1}{\rho}\alpha\Delta t\frac{\partial\overline{p}^{n+1}}{\partial x_i} \tag{2.10}$$

Next, the divergence of Eq. (2.10) is taken and the continuity requirement is imposed for the face velocities (obtained by using linear interpolation on time level $n+1$). Finally, we arrive at:

$$\frac{\partial^2\overline{p}^{n+1}}{\partial x_i\partial x_i} = \frac{\rho}{\Delta t\alpha}\frac{\partial\overline{u}_{i,f}^*}{\partial x_i} \tag{2.11}$$

The numerical procedure is summarized as follows [7]:

1. Solve the filtered Navier-Stokes equations for $\overline{u}$, $\overline{v}$ and $\overline{w}$.
2. Create an intermediate velocity field from Eq. (2.10).
3. The poisson equation of (2.11) is solved using an efficient multi grid solver [8].
4. Compute the face velocities (which satisfy continuity) from the pressure and the intermediate velocity as:

$$\overline{u}_{i,f}^{n+1} = \overline{u}_{i,f}^{n} - \frac{1}{\rho}\alpha\Delta t\left(\frac{\partial P^{n+1}}{\partial x_i}\right)_f \tag{2.12}$$

5. Steps 1 to 4 are performed repeatedly until convergence is reached.
6. Turbulent viscosity is computed.
7. Next time step.

2.4.1 Time advancement

Time advancement is an important issue in large eddy simulations both in the numerical restrictions and the issues regarding the turbulence itself. There are three time-scales that should be taken care of. The first is the stability limit with respect to the numerical scheme involved which can be formulated using the Courant Fredrisch Levy, or CFL for short, condition ($\Delta t = CFL\Delta x\,/u$). The second is called viscous condition that requires the time step to be $\Delta t_\nu = \sigma\Delta y^2/\nu$ where σ depends on the time advancement

technique used (eg. Crank-Nicolson or Runge-Kutta). The last condition expresses the physical importance of the time advancement with respect to the turbulence scales that are going to be resolved. This is expressed as: $\tau = \Delta x/U_c$ and U_c is the convective velocity that has to be chosen to be a characteristic velocity of the order of the free stream velocity, as an example.

Chapter 3

Near wall modeling for LES using TBLE

3.1 Introduction

As it was pointed out in the introduction, LES is incapable to resolve wall encountered flows unless on a reasonably fine mesh, which makes it very expensive for many computational applications. It was also mentioned that this problem can be solved with reasonable accuracy using wall models for some problems. In this chapter a special wall model which is based on boundary layer approximations is presented. We refer to these equations as TBLE here after for convenience.

3.2 Turbulent boundary layer equations

TBLE equations are based on boundary layer assumptions. According to these assumptions, viscous derivatives in the stream-wise and span-wise directions are neglected and the pressure is assumed to be constant in the wall normal direction. This latter approximation implies that the pressure gradient in TBLE cells can be approximately replaced by that of the outer flow in their interface. Applying these simplifications to Navier-Stokes equations we get:

$$\frac{\partial \widetilde{u}_i}{\partial t} + \frac{\partial (\widetilde{u_i u_j})}{\partial x_j} = -\frac{\partial P_m}{\partial x_i} + \nu \frac{\partial^2 \widetilde{u}_i}{\partial y^2}, \quad (i = 1, 3) \tag{3.1}$$

Where $\widetilde{u}_2$ is found from the continuity equation:

$$\widetilde{u}_2 = -\int_0^y \frac{\partial \widetilde{u}_i}{\partial x_i} dy', \quad (i = 1, 3) \tag{3.2}$$

In these equations $\sim$ represents spatial or time filtering. As usual for turbulent calculations, the term $\widetilde{u_i u_j}$ is to be modeled and we can approximate it as we do in RANS. The $\widetilde{u_i u_2}$ component of this term is modeled as:

$$\widetilde{u_i u_2} - \widetilde{u}_i \widetilde{u}_2 \sim -\nu_t \frac{\partial \widetilde{u}_i}{\partial y} \tag{3.3}$$

The remaining terms are simply chosen to be:

$$\frac{\partial(\widetilde{u_i u_1})}{\partial x} \sim \frac{\partial(\widetilde{u}_i \widetilde{u}_1)}{\partial x}, \quad \frac{\partial(\widetilde{u_i u_3})}{\partial z} \sim \frac{\partial(\widetilde{u}_i \widetilde{u}_3)}{\partial z} \tag{3.4}$$

According to [9], adding eddy viscosity models for these terms would not change the statistics very much. Adding these terms and substituting them in Eq. (3.1) yields:

$$\frac{\partial \widetilde{u}_i}{\partial t} + \frac{\partial(\widetilde{u}_i \widetilde{u}_j)}{\partial x_j} + \frac{\partial P_m}{\partial x_i} = \frac{\partial}{\partial y}\left[(\nu + \nu_t)\frac{\partial \widetilde{u}_i}{\partial y}\right], \quad (i = 1, 3) \tag{3.5}$$

Eq. (3.5) is the governing equation we intend to use to provide LES with a boundary condition. In Eq. (3.5) P_m is the pressure which is calculated from the outer LES solved flow. This pressure gradient is fixed in TBLE equations which greatly simplifies our calculations and cuts off many of the usual pressure calculations that exist in hybrid RANS-LES methods.

3.3 Grid used for solving TBLE

TBLE is solved on a grid embedded in the first LES cell. A schematic of the grid is shown in Fig. 3.1. As it is shown in this figure, the first LES node is subdivided into a number of cells. These embedded cells serve as the mesh we need to solve Eq. (3.5) using control volume approach. In order for the first node to be located below $y^+ = 1$, a simple stretching is performed in the wall normal direction. In our calculations, number of nodes necessary to solve TBLE were fixed to 30 which seems to be sufficient for high Reynolds number simulations.

3.4 Boundary conditions for TBLE

On the wall, the usual no-slip boundary condition is employed, while on the last node of TBLE the values from the first LES node are directly taken

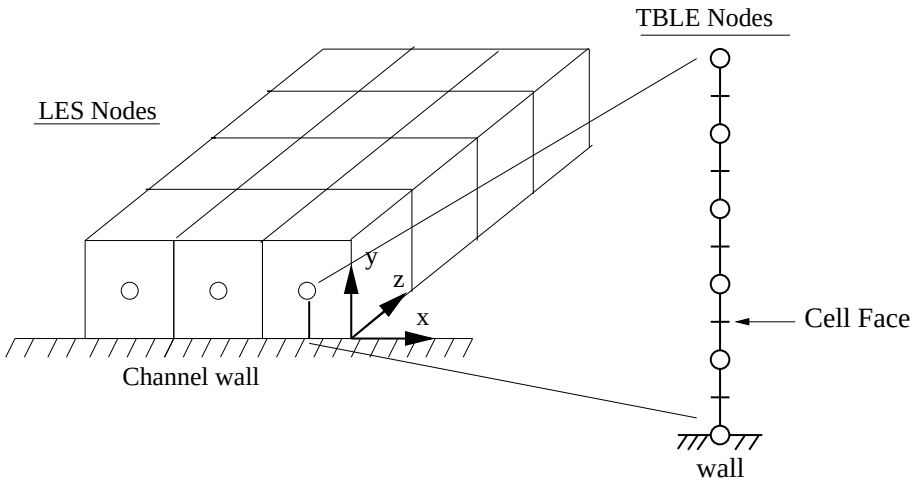

Figure 3.1: Schematic of the computational strategy

as boundary conditions both for u and w equations. This can be shown in the following notation:

$$\widetilde{u}_i(0) = 0, \quad \widetilde{u}_i(y_m) = U_{mi} \tag{3.6}$$

Where U_{mi} is the velocity component in the first node of the LES computation. In the case where we use a one equation model to approximate the eddy viscosity in the TBLE, a boundary condition for the kinetic energy is needed. This boundary condition is set to zero at the wall and equal to the LES kinetic energy at the first LES node.

3.5 Boundary conditions for LES

Two types of boundary conditions are passed from TBLE to LES. The first one is the shear stress at the wall which is predicted by TBLE, and is passed to LES in form of an eddy viscosity. The formulation is as follows:

$$\nu_\tau \frac{U_{LES}}{y_{LES}} = \tau_{wall} \tag{3.7}$$

The other value that is passed to LES is the kinetic energy needed for calculation of the eddy viscosity in the core LES region. If kinetic energy is also solved in the TBLE calculations the calculated values of kinetic energy is then volume averaged over each column of TBLE grids and is passed to the LES solver as a boundary condition for solving subgrid scale kinetic energy equation for its first off-wall node.

If kinetic energy is not solved in TBLE, then the boundary condition is predicted using the following relation (according to [6]):

$$K = C_{\mu}^{-0.5} U_{*}^{2} \tag{3.8}$$

3.6 Eddy viscosity formulation

Three different formulations are used for eddy viscosity calculation. These formulations differ from a range of different zero equation models to a one equation model as follows:

1. A zero equation model with Van-Driest damping function. This formulation can be represented as:

$$\frac{\nu_t}{\nu} = y^{+}\kappa \left[1 - exp(-y^{+}/A)\right]^2 \tag{3.9}$$

   Where $\kappa = 1/e \sim 0.41$, $A = 19$ and $y^{+} = u_{\tau} y/\nu$ is the distance from the wall, in wall units.

2. A zero equation model based on the following formulation:

$$\begin{aligned} \nu_t &= (C \times S_{\mu})^2 \times S \\ S_{\mu} &= \kappa \times y \times f_{\mu} \\ S &= \sqrt{\widetilde{S_{ij}}\widetilde{S_{ij}}} \\ f_{\mu} &= \tanh\left[\frac{1}{4}\left(\frac{\mu_t}{\mu}\right)^{0.33}\right] \\ C &= 0.9, \quad \kappa = 0.41 \end{aligned} \tag{3.10}$$

3. A one equation model based on [10]. The formulation is as follows:

$$\frac{\partial K}{\partial t} + \frac{\partial(\widetilde{u_j} K)}{\partial x_j} = \frac{\partial}{\partial y}\left[(\nu + \nu_t)\frac{\partial K}{\partial y}\right] + P_k - C_{\epsilon}\frac{K^{3/2}}{l} \tag{3.11}$$

   where, the corresponding parameters are:

$$\begin{aligned} P_k &= 2\widetilde{S_{ij}}\widetilde{S_{ij}} \\ l &= y\left[1 - \exp\left(-A_l \frac{k^{1/2} y}{\nu}\right)\right] \\ \nu_t &= C_{\mu} k^{1/2} y \left[1 - \exp\left(-A_{\mu}\frac{k^{1/2} y}{\nu}\right)\right] \\ C_{\epsilon} &= 0.416, \quad C_{\mu} = 0.22, \quad A_{\mu} = 0.016, \quad A_l = 0.263 \end{aligned} \tag{3.12}$$

The last two terms in Eq. (3.11) are the production and dissipation of kinetic energy respectively.

3.7 Numerical method

Control volume approach is used to solve Eq. (3.5) numerically. Here only the derivations for the x direction equation will be presented. Assuming a cartesian grid, Eq. (3.5) can be written in x direction as:

$$\frac{\partial \widetilde{u}}{\partial t} + \frac{\partial(\widetilde{u}\widetilde{u}_j)}{\partial x_j} + \frac{\partial P_m}{\partial x} = \frac{\partial}{\partial y}\left[(\nu + \nu_t)\frac{\partial \widetilde{u}}{\partial y}\right] \tag{3.13}$$

Integration of Eq. (3.13) yields:

$$\int_V \int_t^{t+\Delta t} \frac{\partial \widetilde{u}}{\partial t} dV dt + \int_V \int_t^{t+\Delta t} \frac{\partial(\widetilde{u}\widetilde{u}_j)}{\partial x_j} dV dt + \int_V \int_t^{t+\Delta t} \frac{\partial P_m}{\partial x} dV dt = \int_V \int_t^{t+\Delta t} \frac{\partial}{\partial y}\left[(\nu + \nu_t)\frac{\partial \widetilde{u}}{\partial y}\right] dV dt \tag{3.14}$$

3.7.1 Spatial discretization

Integrating Eq. (3.14) further and assuming pressure to be constant across the boundary layer, we will have:

$$\begin{aligned} \left(\widetilde{u}_p - \widetilde{u}_p^{\circ}\right) \Delta V &= S_u \Delta V \Delta t + \int_V \int_t^{t+\Delta t} \frac{\partial}{\partial y}\left[(\nu + \nu_t)\frac{\partial \widetilde{u}}{\partial y}\right] dV dt \\ S_u &= -\frac{\partial P_m}{\partial x} - \frac{1}{\Delta V}\int_V \frac{\partial(\widetilde{u}\widetilde{u}_j)}{\partial x_j} dV \end{aligned} \tag{3.15}$$

where, the convective term has been explicitly integrated and imposed in the S_u term. Also, $\widetilde{u}_p^{\circ}$ is the value of velocity obtained at node P in the old time step. Integration of the diffusion term yields:

$$\begin{aligned} \left(\widetilde{u}_p - \widetilde{u}_p^{\circ}\right) \Delta V &= S_u \Delta V \Delta t + \left\{\left[(\nu + \nu_t)\frac{\partial \widetilde{u}}{\partial y}\right]_n - \left[(\nu + \nu_t)\frac{\partial \widetilde{u}}{\partial y}\right]_s\right\} \Delta x \Delta z \Delta t \\ S_u &= -\frac{\partial P_m}{\partial x} - \frac{1}{\Delta V}\int_V \frac{\partial(\widetilde{u}\widetilde{u}_j)}{\partial x_j} dV \end{aligned} \tag{3.16}$$

Now we divide by Δt and discretize the derivatives using central differences:

$$\begin{aligned} \left(\widetilde{u}_p - \widetilde{u}_p^{\circ}\right) a_{\circ} &= S_u \Delta V + \left[D_n\left(\widetilde{u}_N - \widetilde{u}_P\right) - D_s\left(\widetilde{u}_P - \widetilde{u}_S\right)\right] \Delta x \Delta z \\ S_u &= -\frac{\partial P_m}{\partial x} - \frac{1}{\Delta V}\int_V \frac{\partial(\widetilde{u}\widetilde{u}_j)}{\partial x_j} dV \\ D_n &= \left(\frac{\nu + \nu_t}{\delta y}\right)_n, \quad D_s = \left(\frac{\nu + \nu_t}{\delta y}\right)_s, \quad a_{\circ} = \frac{\Delta V}{\Delta t} \end{aligned} \tag{3.17}$$

where n and s subscripts, denote the north and south face values in the control volume approach, while N, S and P denote the nodal values of north south and P nodes.

3.7.2 Time discretization

Up to here, all the variables are considered to be evaluated at the current time step. This gives us a first order accuracy in time and an implicit scheme. But, in the numerical code developed, the discretization used for time in the numerical procedure is capable of providing both first and second order, Crank-Nicolson method, to the user. It is easy to implement such a variable formulation for time discretization through the introduction of the variable α as follows (see [11]):

$$\begin{aligned}\left(\widetilde{u}_p - \widetilde{u}_p^\circ\right) a_\circ = S_u \Delta V \quad &+ \quad \left[\alpha D_n \left(\widetilde{u}_N - \widetilde{u}_P\right) + (1-\alpha) D_n \left(\widetilde{u}_N^\circ - \widetilde{u}_P^\circ\right)\right] \Delta x \Delta z \\ &- \quad \left[\alpha D_s \left(\widetilde{u}_P - \widetilde{u}_S\right) - (1-\alpha) D_s \left(\widetilde{u}_P^\circ - \widetilde{u}_S^\circ\right)\right] \Delta x \Delta z\end{aligned} \tag{3.18}$$

where all the terms indicated by $\circ$ are from the old time step and will be put later in the source term S_u. Doing so we will have:

$$\begin{aligned} a_P \widetilde{u}_p &= a_N \widetilde{u}_N + a_S \widetilde{u}_S + S_u \Delta V \\ a_N &= \alpha D_n \Delta x \Delta z \\ a_S &= \alpha D_s \Delta x \Delta z \\ a_P &= a_\circ + \alpha D_n \Delta x \Delta z + \alpha D_s \Delta x \Delta z = a_\circ + a_N + a_S \\ S_u &= -\frac{\partial P_m}{\partial x} \Delta V - \int_V \frac{\partial (\widetilde{u}\widetilde{u}_j)}{\partial x_j} dV \\ &+ (1-\alpha) \Delta x \Delta z \left[D_n \left(\widetilde{u}_N^\circ - \widetilde{u}_P^\circ\right) - D_s \left(\widetilde{u}_P^\circ - \widetilde{u}_S^\circ\right)\right] + a_\circ \widetilde{u}_p^\circ \end{aligned} \tag{3.19}$$

All the convective parts in Eq. (3.5) are modeled explicitly. This approach is chosen to decrease the numerical effort. Also, in all the simulations carried out here, the Crank-Nicolson method is used as time discretiztion by setting $\alpha = 0.5$.

Chapter 4

Channel flow simulations

4.1 Introduction

Derivation of equations of TBLE was discussed in the previous chapters. This method was applied for a number of fully developed channel flow large eddy simulations. The purpose of the simulations was to determine the capabilities of this method. However, it was known to us that the method would give reasonable results for an attached flow such as a channel flow. Therefore a lot of efforts were put to find better solutions and probably a better understanding of the weaknesses of the method. All the simulations were compared to the log-law velocity profile.

4.2 Domain specification and LES nodes

Channel domain and the corresponding grid points are shown in table 4.1. Different Reynolds numbers are also indicated in this table. To fix matching point, stretching is used in the LES grid and the corresponding stretching factor is also mentioned.

4.3 Different Reynolds numbers

In this section, the scheme is used for simulation of flows with different Reynolds numbers based on the friction velocity, U_* and the channel half-width, δ, which is one. Simulations are done for $Re_\tau = 2000$, $Re_\tau = 4000$ and $Re_\tau = 8000$. Fig. 4.1 shows the velocity profiles obtained for these Reynolds numbers. The results loose their accuracy as the Reynolds number is increased. This is due to the fact that number of LES nodes is kept constant

Table 4.1: Domain specification and number of LES grid nodes

Re_τ	$(x \times y \times z)_{max}$	Stretching Factor	y_m^+	$(I \times J \times K)_{max}$
2000	6.4×2×3.2	1.00	30.3	34×66×34
4000	6.4×2×3.2	1.04	30.0	34×66×34
4000	6.4×2×3.2	1.03	40.0	34×66×34
4000	6.4×2×3.2	1.01	50.0	34×66×34
4000	6.4×2×3.2	1.03	60.0	34×50×34
8000	6.4×2×3.2	1.08	30.0	34×66×34

for different simulations. Therefore, the poor grid quality on the LES side can not provide solutions at higher Reynolds numbers as accurate as in lower Reynolds numbers. The deviation starts from $y^+ > 30$ which is the matching point between LES and TBLE. The deviation imposes a downward shift on the velocity profile. It is interesting to point out the fact that, when the matching point is increased. eg. from $y^+ = 30$ to $y^+ = 60$, the velocity profile shifts up. This is further discussed in the next section.

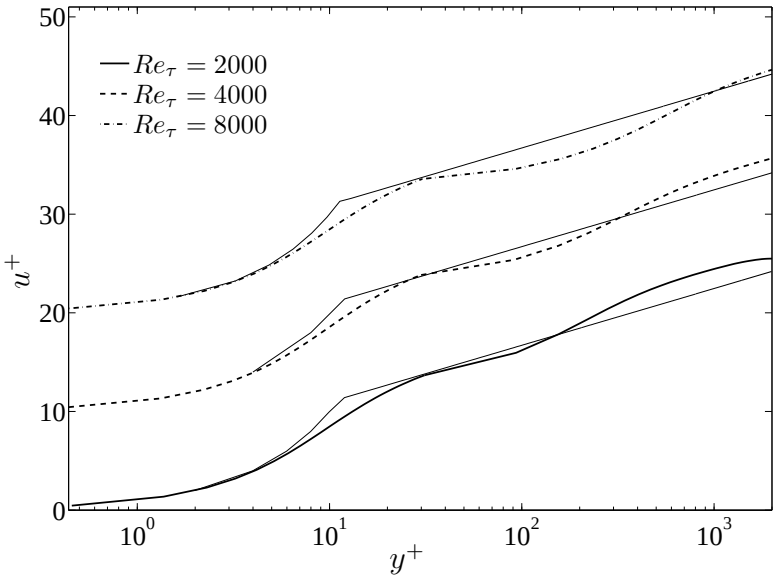

Figure 4.1: Velocity profiles for different Reynolds numbers - Re_τ, $y_m^+ = 30$

4.4 Matching point specification

An important issue when using hybrid schemes for LES, is to specify a matching point for the two schemes. Here, different matching points (y_m^+) are assumed and the results are shown in Fig. 4.2. The intension here is to put the matching point somewhere out of the viscous sublayer. We know that it should be somewhere with $y_m^+ > 30$ where, viscosity effects are gone. It is better to place it well outside this limit but other issues are to be considered and a compromise leads us to the final decision. As it is seen in Fig. 4.2 a suitable position should be $y^+ = 50$ or $y^+ = 60$. It is observed that the results become better by increasing y_m^+ this is due to the fact that when we go further out from the viscous sublayer the effect of viscosity is more and more vanished. As it was pointed out previously, for higher Reynolds numbers and when the matching point is taken to be farther away from the surface the results get better. This could be due to the fact that better shear stress is provided by TBLE to LES because of a better position of the matching point.

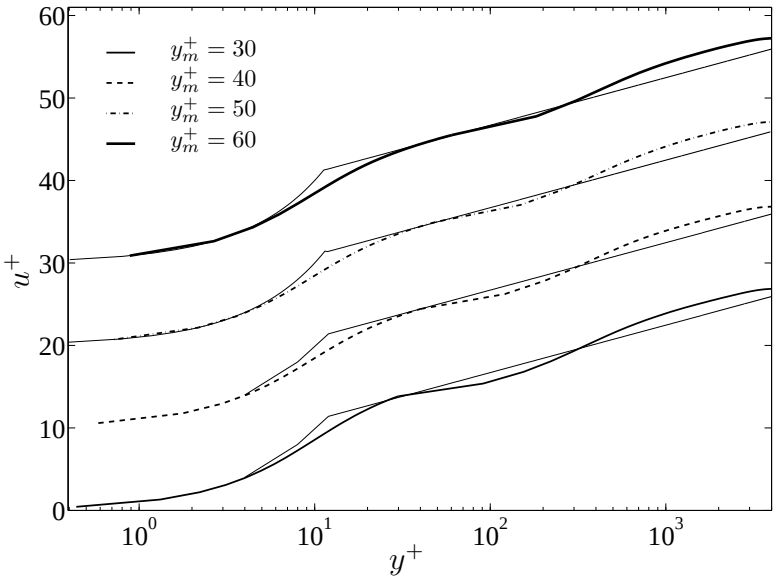

Figure 4.2: Velocity profiles for different matching points - $Re_\tau = 4000$

4.5 Choice of eddy viscosity model

At the very beginning it was assumed that the choice of eddy viscosity model in the TBLE region would result in different velocity profiles. But it turned out later that there is no big difference, at least in the accuracy of the velocity profiles. This is shown in Figs. 4.3 and 4.4. Therefore, no further conclusion can be drawn. One reason could be the simplicity of the geometry which makes the need of a more sophisticated modeling redundant. The other could be that the eddy viscosity calculated from the zero equation models are very well tuned for this case and if a more difficult case is studied the difference would show up. This is pointed out in reference [12] where it is shown that the shear stress computed using a zero equation model could be over predicted and a dynamic adjustment of the damping function appears to be necessary. On the other hand, the one equation model used here is compatible with the one used in the LES solver and it has some advantage in other flow cases.

4.6 Importance of different terms

It is a very important issue to know the importance of different terms in TBLE equations. Here, the investigation was started by only considering the diffusion term in TBLE equations and then adding the pressure term and the convective term later. It was observed that adding these extra terms to the governing equations would not lead to considerable change in the velocity profile, at least for our current channel flow. The result is shown in Fig. 4.5 which shows the same conclusion. It can be seen that the most dominant term is the diffusion term. Therefore, it seems very reasonable for the results to be independent of the choice of including or excluding the convective term. The other point is the insignificance of the pressure gradient which can play a big role in simulations involving large pressure variations.

4.7 TBLE and additional computational time

It has been proven that the combination of TBLE and LES is much cheaper than a wall resolved LES. In this section CPU time used for different simulations described here is discussed regardless of the quality of the results. The results are shown in table 4.2. It was assumed that a fully resolved LES is indeed much more expensive than the current approach, therefore the table does not include the data of such a simulation. What is shown in the column *CPU time per iteration in seconds* is the time spent in each iteration

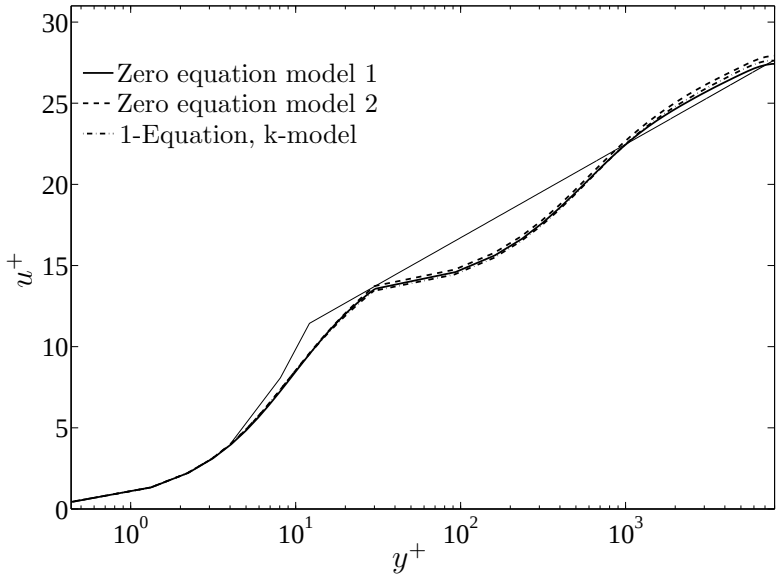

Figure 4.3: Velocity profiles for different eddy viscosity models - $Re_\tau = 8000$, $y_m^+ = 30$

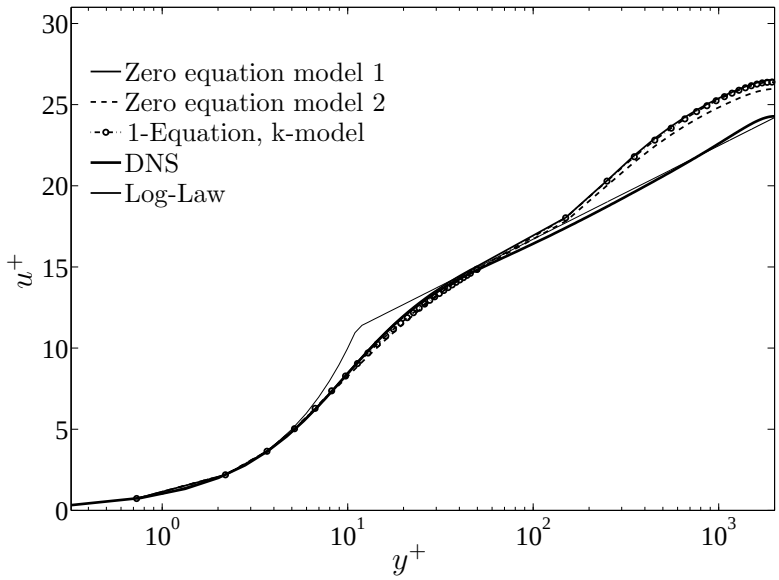

Figure 4.4: Velocity profiles for different eddy viscosity models - $Re_\tau = 2000$, $y_m^+ = 50$

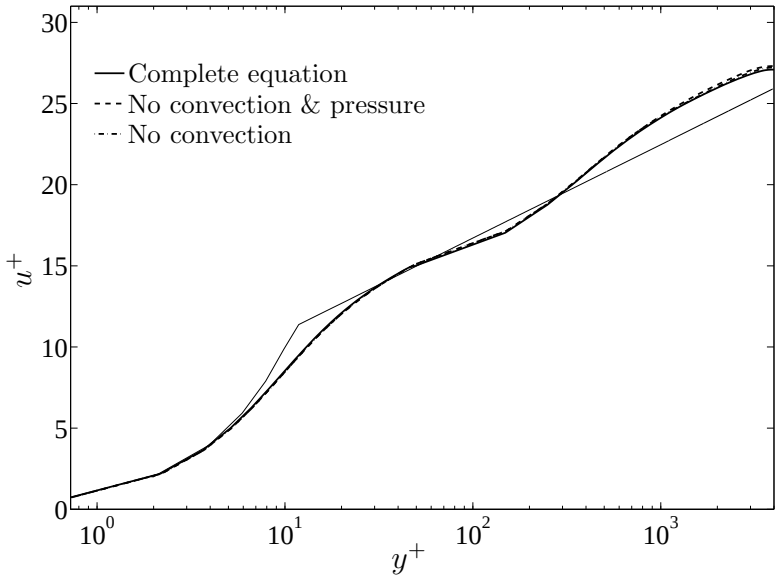

Figure 4.5: Velocity profiles for different versions of TBLE scheme - $Re_\tau = 4000$

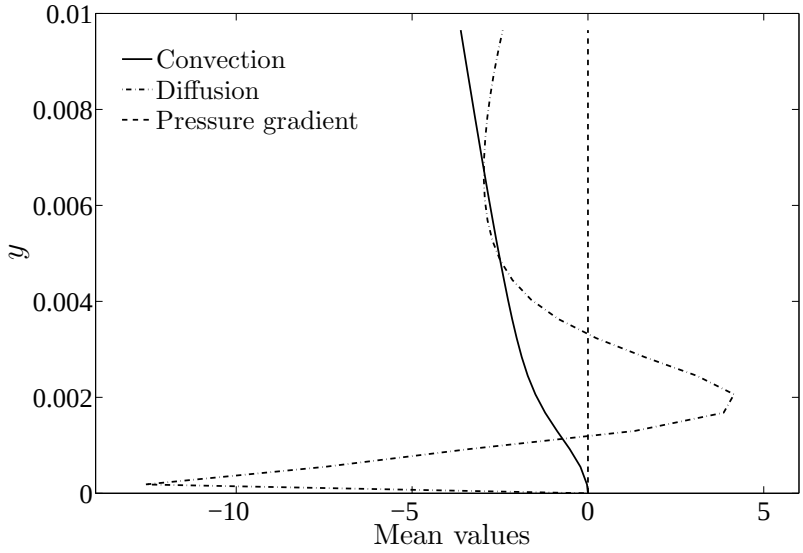

Figure 4.6: Different terms in Eq. (3.1) - $Re_\tau = 4000$

Table 4.2: CPU time comparison

Re_τ	Eddy viscosity model	y_m^+	CPU time per iteration in seconds
2000	Zero Equation Model I	30.3	0.45
2000	Zero Equation Model II	30.0	0.48
2000	Zero Equation Model II (Sub. Iter.)	30.0	0.84
2000	One Equation Model	50.0	0.71
4000	Zero Equation Model I	30.3	0.65
4000	Zero Equation Model II	30.0	0.8
4000	One Equation Model	50.0	0.92
8000	Zero Equation Model I	30.0	0.7
8000	Zero Equation Model II	30.0	0.67
8000	One Equation Model	30.0	0.82

of a time step, every time step consists of several iterations. It was observed, according to table 4.2, that as it was expected, using a one equation model for calculation of the eddy viscosity has an impact on the CPU time spent in every iteration. It is also observed that the matching point has also an effect that could be minor.

Another point that has to be emphasized on is that since the shear stress at the wall depends on the velocity and the velocity calculated from TBLE also depends on the shear stress at the wall implicitly, it seems that some iterations has to be made, in order to make velocity and shear stress consistent. The impact of this extra iterations is shown in the table for the case of zero equation model II in the column followed by *Sub. Iter.* in the parentheses. Here we find that the effect of such an extra work is significant, while it does not make any difference in terms of accuracy.

Chapter 5

Other hybrid methods

5.1 Introduction

Using turbulent simplified boundary layer equations as a wall model for large eddy simulations is a subcategory of a general category called hybrid methods. In this chapter other hybrid methods are discussed very briefly.

5.2 Detached eddy simulations

The advent of Hybrid RANS-LES methods could be traced back to Detached Eddy Simulations (DES) which were introduced by Spalart[13] in 1997. The method is based on a mixture of RANS and LES where attached boundaries are solved using the one equation Spalart-Allmaras RANS and separated parts of the flow are solved using LES. The LES in the core region uses the one equation SGS model by switching the length scale to the local grid spacing. The idea behind such a reasoning is that in the attached flow areas, where a well-tuned RANS gives good results, there is no need to use an expensive LES, while in the areas where large scales are present and especially in the areas where separation happens, where LES is well-known to handle better, LES is used. This approach leads to a considerable reduction in the computational expenses. Lots of good performance of such an approach is reported in the literature (eg. [14] and [15]). On the contrary, it has been found that such an approach does not give good results for attached flows [16].

5.3 Hybrid RANS-LES methods

As it was described in the previous section, DES has already opened the way for such hybrid methods. But why is a hybrid method necessary? The answer is described below:

It is well known that in order to resolve the near wall turbulence correctly, we need to have fine grid in normal as well as transverse and longitudinal directions. For example, the wall normal resolution should be $y^+ = 1$ in wall units. Also $\Delta x^+ = 100$ (streamwise) and $\Delta z^+ = 20$ (spanwise). This resolution demanding characteristic of LES is a big draw-back for its application. While RANS methods have the same restriction in wall normal direction, they do not have such restrictions in other directions. This is very convenient in terms of implementation for different applications but RANS proves to be not good in separated flow predictions. Therefore, a blend of the two methods could be very successful.

One important thing about hybrid methods is the specification of matching points between the two methods. The matching point should be placed in the logarithmic part of the boundary layer where the flow is fully turbulent and coarse grid spacing in planes parallel to the walls is adequate for LES, since the grid spacing is determined by the requirement of resolving the mean flow rather than resolving the near wall turbulent process that is going on. While successful in simulation of different flow problems, there exists some shortcomings and difficulties. For example when using hybrid RANS-LES approach for turbulent channel flow, if one compares the modeled turbulent kinetic energy, it could be observed that while in the RANS region the modeled kinetic energy agrees well with the reality, the resolved kinetic energy is as large as the modeled one. Therefore, the total kinetic energy is much larger than its actual value.

5.4 Dynamic wall modeling using TBLE

In the simulations reported in the literature it is often pointed out that when using TBLE as a wall model and in complex geometries, the shear stress provided to LES is often over predicted. Wang and Moin [12] proposed a dynamic wall modeling based on equating the unresolved portions of the stresses in the matching point interface using the following formulation:

$$\langle \nu_{sgs} \rangle = \kappa \left\langle y_w^+ \left(1 - e^{(-y_w^+/A)}\right)^2 \right\rangle \tag{5.1}$$

From Eq. (5.1) κ can be found to be

$$\kappa = \langle \nu_{sgs} \rangle \Big/ \left\langle y_w^+ \left(1 - e^{(-y_w^+/A)}\right)^2 \right\rangle \tag{5.2}$$

where, <> denotes averaging in a homogenous direction and over a few hundred time steps. This is done to smooth the data. A problem that arises in this kind of modeling is the fact that the velocities at the first off-wall LES nodes are not well defined and the eddy viscosity that is calculated based on them is not reliable for computations as well. A remedy for this is to use the velocities at the second off-wall LES nodes as the reference for computations as is pointed out in [12].

Chapter 6

Future work and unfinished simulations

6.1 Introduction

Although, only channel flow simulations were foreseen for the current study, the promising results obtained in the course of the project brought this idea up to make simulations over more complicated geometries to put the method to further test. In this regards, flow over a two-dimensional bump was the first test case. The first step to perform the simulation was to generate a mesh suitable for large eddy simulations that could have orthogonality properties as well.

At the end we were successful to make simulations with the generated grid in the hybrid mode but the results needed further attention and correction which time did not allow us to accomplish. This chapter is an asset to this work for the interested reader to follow the work on his/her own.

What is discussed here in this chapter is grid generation using elliptic partial differential equations, in brief, followed by a description of the problem of the two-dimensional bump (see [17]). The purpose of the chapter is to show how to make grid over a pre-defined set of boundary nodes and it is demonstrated how to add certain characteristics such as boundary orthogonality to the grid. The grid could be further used for simulations with geometries other than the simple channel.

6.2 Poisson equations for grid generation

Numerical grid generation is far different from the algebraic grid generation in the sense that a set of partial differential equations (PDE) has to

be solved in order to generate a grid. The advantage of doing so would be a smoother grid which also has better characteristics needed for a reliable CFD simulation.

Poisson equations are often used for numerical grid generation. These equations provide a flexible way for grid generation with orthogonality at the boundaries which is important for CFD applications. Poisson equations used here are:

$$\xi_{xx} + \xi_{yy} = P \tag{6.1}$$
$$\eta_{xx} + \eta_{yy} = Q \tag{6.2}$$

In order to solve the equations using finite differences,the equations have to be transformed into a computational space where the discretization is carried out. After the transformation, the equations become:

$$\alpha x_{\xi\xi} - 2\beta x_{\xi\eta} + \gamma x_{\eta\eta} = -J^2 \left(P x_\xi + Q x_\eta\right) \tag{6.3}$$
$$\alpha y_{\xi\xi} - 2\beta y_{\xi\eta} + \gamma y_{\eta\eta} = -J^2 \left(P y_\xi + Q y_\eta\right) \tag{6.4}$$

where:

$$\alpha = x_\eta^2 + y_\eta^2 \tag{6.5}$$
$$\beta = x_\xi x_\eta + y_\xi y_\eta \tag{6.6}$$
$$\gamma = x_\xi^2 + y_\xi^2 \tag{6.7}$$

P and Q are used as forcing terms to make grids orthogonal at the boundaries and to cluster them near surfaces where we have boundary layers and more grid nodes are needed (See also [18] or [19]). J is the jacobian of the transformation which is:

$$J = x_\xi y_\eta - x_\eta y_\xi \tag{6.8}$$

Other metrics of the transformation are defined as follows:

$$\begin{aligned} \xi_x &= \frac{y_\eta}{J} \\ \xi_y &= -\frac{x_\eta}{J} \\ \eta_x &= -\frac{y_\xi}{J} \\ \eta_y &= \frac{x_\xi}{J} \end{aligned} \tag{6.9}$$

Elliptic equations need specified boundary conditions for all boundaries. Therefore all the nodes at all the boundaries should be fixed and pre-determined.

Solving Eqs. (6.3) and (6.4) using Eqs. (6.5) to (6.9) with specified boundary conditions (nodes on the boundaries) generates a mesh that is not orthogonal to the boundaries. In order to have orthogonality on the surfaces, the following restrictions on the forcing terms has to be applied [18]:

$$\begin{aligned} P(\xi,\eta) &= p(\xi)e^{-a\eta} + r(\xi)e^{-c(\eta_{max}-\eta)} \\ Q(\xi,\eta) &= q(\xi)e^{-b\eta} + s(\xi)e^{-d(\eta_{max}-\eta)} \end{aligned} \tag{6.10}$$

where p, q, r and s are calculated by orthogonality and clustering conditions. We do not mention all the details for the sake of brevity and only the final equations are mentioned:

$$p(\xi) = \left[\frac{y_\eta R_1 - x_\eta R_2}{J}\right]_{k=1} \tag{6.11}$$

$$q(\xi) = \left[\frac{-y_\xi R_1 + x_\xi R_2}{J}\right]_{k=1} \tag{6.12}$$

where:

$$R_1 = \left[\frac{-\left(\alpha x_{\xi\xi} - 2\beta x_{\xi\eta} + \gamma x_{\eta\eta}\right)}{J^2}\right]_{k=1} \tag{6.13}$$

$$R_2 = \left[\frac{-\left(\alpha y_{\xi\xi} - 2\beta y_{\xi\eta} + \gamma y_{\eta\eta}\right)}{J^2}\right]_{k=1} \tag{6.14}$$

A similar set of equations can be applied for the other boundary where $\eta = \eta_{max}$, which are:

$$r(\xi) = \left[\frac{y_\eta R_3 - x_\eta R_4}{J}\right]_{k=k_{max}} \tag{6.15}$$

$$s(\xi) = \left[\frac{-y_\xi R_3 + x_\xi R_4}{J}\right]_{k=k_{max}} \tag{6.16}$$

where:

$$R_3 = \left[\frac{-\left(\alpha x_{\xi\xi} - 2\beta x_{\xi\eta} + \gamma x_{\eta\eta}\right)}{J^2}\right]_{k=k_{max}} \tag{6.17}$$

$$R_4 = \left[\frac{-\left(\alpha y_{\xi\xi} - 2\beta y_{\xi\eta} + \gamma y_{\eta\eta}\right)}{J^2}\right]_{k=k_{max}} \tag{6.18}$$

Now we have all the ingredients needed. The next step is to discretize equations using finite differences and use line-SOR[1] method to solve the discretized equations. Equations are solved for x and y.

[1]Successive Over Relaxation

6.3 Two-dimensional bump geometry

The two-dimensional hill geometry is shown in Fig. 6.1. The geometry dimensions are:

$$L_2/H = 8.86 \quad h/H = 0.46, \quad L_1/H = 0.41, \quad (L_2 - L1)/H = 0.81, \quad H = 0.3\,(m)$$
$$-0.61/2 < z/H < 0.61/2$$

where $2z = 0.61$ is the width of the channel in z direction (not shown in the figure). It has to be mentioned that TBLE equations need to be solved in a

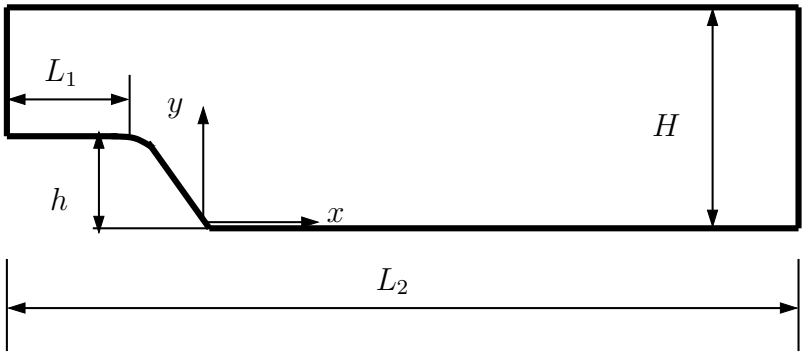

Figure 6.1: Schematic of the Problem

body-fitted coordinate system. The boundary conditions and the method of solving TBLE equations remain the same as was described in the previous chapters. The inlet boundary condition for LES is obtained from a RANS simulation, which is done before. The dynamic model of [12] proves to be necessary. Also, averaging over a few iterations for the pressure gradient passed by LES to TBLE is a necessity in the simulations.

6.4 Conclusion

In this work, a hybrid method was introduced which uses simplified turbulent boundary layer equations to provide LES simulations with approximate wall boundary conditions. Here, we successfully applied this hybrid method to fully developed turbulent channel flow simulations and the results were in good agreement with Log-law velocity profile. Comparison between data from DNS was also performed for one case and the result was satisfactory.

Simplified turbulent boundary layer equations that were used were applied in different ways. In the simplest form, only the diffusion and time derivative terms were considered. Later on, the pressure gradient term and the convective terms were added. It was observed that for the fully developed channel flow simulations including or excluding these two latter terms does not change the results very much. The effect of intermediate iterations were considered to make eddy viscosity and velocity more consistent in the TBLE region and it was observed, as is also reported in the literature, that it does not make considerable difference.

Also different eddy viscosity models were used for TBLE equations. Two zero equation models and a one equation model were tested and it was observed that the choice of eddy viscosity does not affect the solution. A CPU time comparison between using TBLE with each of the eddy viscosity models was also performed. At the end some proposals for continuation of this research, by applying the method to a different flow geometry, was proposed.

Bibliography

[1] L. Davidson, D. Cokljat, J. Fröhlich, M.A. Leschziner, C. Mellen, and W. Rodi, editors. *LESFOIL: Large Eddy Simulation of Flow Around a High Lift Airfoil*, volume 83 of *Notes on Numerical Fluid Mechanics*. Springer Verlag, 2003.

[2] J.S. Baggett, J. Jiménez, and A.G. Kravchenko. Resolution requirements in large eddy simulations of shear flows. In *Annual Research Briefs*, pages 51–66, Center for Turbulent Research, Stanford Univ./NASA Ames Reseach Center, 1997.

[3] J.W. Deardorff. A numerical study of the three-dimensional turbulent channel flow at large Reynolds numbers. *Journal of Fluid Mechanics*, 41:453–480, 1970.

[4] L. Davidson and S.-H. Peng. Hybrid LES-RANS: A one-equation SGS model combined with a $k - \omega$ model for predicting recirculating flows. *International Journal for Numerical Methods in Fluids*, 43:1003–1018, 2003.

[5] L. Davidson. Hybrid LES-RANS: Estimating resolution requirements using two-point correlations and spectra. ERCOFTAC Bullentin, Special Issue on *Wall modelling in LES*, pp. 19–24, March, 2007.

[6] L. Davidson and B. Farhanieh. CALC-BFC: A finite-volume code employing collocated variable arrangement and cartesian velocity components for computation of fluid flow and heat transfer in complex three-dimensional geometries. Rept. 95/11, Dept. of Thermo and Fluid Dynamics, Chalmers University of Technology, Gothenburg, 1995.

[7] L. Davidson. LES of recirculating flow without any homogeneous direction: A dynamic one-equation subgrid model. In K. Hanjalić and T.W.J. Peeters, editors, *2nd Int. Symp. on Turbulence Heat and Mass Transfer*, pages 481–490, Delft, 1997. Delft University Press.

[8] P. Emvin and L. Davidson. Development and implementation of a fast large eddy simulations method. Rept., Dept. of Thermo and Fluid Dynamics, Chalmers University of Technology, Gothenburg, 1997.

[9] W. Cabot. Near-wall models in large eddy simulations of flow behind a backward-facing step. In *Annual Research Briefs*, pages 199–210, Center for Turbulent Research, Stanford Univ./NASA Ames Reseach Center, 1996.

[10] M. Wolfshtein. The velocity and temperature distribution in one-dimensional flow with turbulence augmentation and pressure gradient. *Int. J. Mass Heat Transfer*, 12:301–318, 1969.

[11] H.K. Versteegh and W. Malalasekera. *An Introduction to Computational Fluid Dynamics - The Finite Volume Method*. Longman Scientific & Technical, Harlow, England, 1995.

[12] M. Wang and P. Moin. Dynamic wall modelling for large eddy simulation of complex turbulent flows. *Physics of Fluids*, 14(7):2043–2051, 2002.

[13] P.R. Spalart, W.-H. Jou, M. Strelets, and S.R. Allmaras. Comments on the feasability of LES for wings and on a hybrid RANS/LES approach. In C. Liu and Z. Liu, editors, *Advances in LES/DNS, First Int. conf. on DNS/LES*, Louisiana Tech University, 1997. Greyden Press.

[14] M. Shur, P.R. Spalart, M. Strelets, and A. Travin. Detached-eddy simulation on an airfoil at high angle of attack. In W. Rodi and D. Laurence, editors, *Engineering Turbulence Modelling and Experiments 4*, pages 669–678. Elsevier, 1999.

[15] M. Strelets. Detached eddy simulation of massively separated flows. AIAA paper 2001–0879, Reno, NV, 2001.

[16] N.V. Nikitin, F. Nicoud, B. Wasistho, K.D. Squires, and P. Spalart. An approach to wall modeling in large-eddy simulations. *Physics of Fluids*, 12(7):1629–1632, 2000.

[17] DESider project – ONERA experimental study – turbulent separated flow on a bump. Technical report, April, 2005.

[18] R.L. Sorenson. A computer program to generate two-dimensional grids about airfoils and other shapes by use of poisson's equation. Report M80-26266, NASA, Moffet Field-California, May 1980.

[19] J.L Steger and R.L. Sorenson. Automatic mesh-point clustering near a boundary in grid generation with elliptic partial differential equations. *J. Comput. Phys.*, 1979.